Int. J. Multiphase Flow Vol. 17, No. 3, pp. 395–413, 1991
Printed in Great Britain.

0301-9322/91 $3.00 + 0.00

EFFECT OF CONTACT FORCES ON SEDIMENTING SPHERES IN STOKES FLOW

M. TABATABAIAN and R. G. COX
Department of Civil Engineering and Applied Mechanics, McGill University, Montreal, Quebec H3A 2K6, Canada

(Received 16 July 1990; in revised form 5 November 1990)

Abstract—The macroscopic behavior of a suspension of sedimenting particles in a fluid is closely related to and depends on the microstructure and relative motion of particles in the suspension. Thus, the calculation of the trajectories of the particles is an essential step in the mathematical modeling of the macroscopic behavior of the suspension. Classical low Reynolds number hydrodynamics predicts that sedimenting solid spherical particles approach one another typically to within 10^{-3} of a radius, indicating that the surface roughness of the particles can become significant and takes part in the interaction process. In this paper, assuming zero Reynolds number flow, the trajectories of two solid spheres sedimenting in either a quiescent fluid or a shear flow are calculated. The cases of ideally smooth and of rough spheres are compared in order to examine the effects of surface roughness on the trajectories.

Key Words: suspension, sedimentation, particle interactions, Stokes flow

1. INTRODUCTION

There have been numerous experimental and theoretical investigations of the macroscopic behavior of a flowing suspension of particles in a fluid, in which the motion is a result of either an applied flow (e.g. shear or extentional flow) or of an external applied force. For example, one might have macroscopic motion of particles due to gravity (e.g. sedimentation), electrical (e.g. electrophoresis) or magnetic fields. The macroscopic properties of such suspensions (e.g. the rheological, optical, electrical, magnetic and heat and mass transfer properties) are related to the microstructure of the suspensions. This may occur in a direct manner in that, for example, particle orientation (Okagawa *et al.* 1973) or the probability of relative positions of particles (Batchelor & Green 1972) may affect the macroscopic viscosity of the suspension or may occur in an indirect manner in that effects on a microscopic scale can result in a flux of the suspended particles on the macroscopic scale, so changing the way the macroscopic concentration of particles varies with position. Thus, in a shear flow, fluxes of particles across the shear flow on the macroscopic scale may occur in a diffusion-like manner due to particle–particle interactions (Karnis *et al.* 1966). Much of the theoretical work that has been undertaken which relates the microscopic behavior of a suspension to its macroscopic properties, has been for very dilute suspensions in which particles can be considered as isolated with no interactions occurring between them. At a slightly higher concentration at which particle interactions play a significant role, it is necessary to investigate particle motion at the microscopic scale. At this scale one may consider two, three or more interacting particles and may include in addition gravity forces, attractive van der Waals forces or repulsive double-layer forces acting on the particles. Classical low Reynolds number hydrodynamics predicts that sedimenting spheres in a shear flow can approach one another typically to within 10^{-3} of a radius. Thus, the particles with surface roughness height (i.e. the height of bumps on the surface) of order 10^{-3} of a radius or larger will make physical contact during their motion when the roughness height becomes equal to the gap width between them. It is assumed that the particles are so small that fluid inertia and particle inertia effects are negligible. For such zero Reynolds number flow, the fluid velocity $\mathbf{u}$ and dynamic pressure p satisfy the creeping flow equations

$$\mu \nabla^2 \mathbf{u} = \nabla p, \quad \nabla \cdot \mathbf{u} = 0, \qquad [1]$$

where μ is the dynamic viscosity of the fluid. The no-slip boundary condition is assumed to apply at the surfaces of the particles and at infinity $\mathbf{u}$ is assumed to approach the undisturbed flow field

(which for the case of sedimentation alone may be taken to be zero). Since these equations and boundary conditions are linear it follows that the rigid-body motion (i.e. the velocities and angular velocities) of the hydrodynamically interacting sedimenting particles must be linearly related to the forces and torques they exert on the fluid.

In a bidisperse suspension (in which one has two species of particles present which sediment at different rates) or in a polydisperse suspension (in which one has many species of particles present all sedimenting at different rates) the most common type of particle interaction will, at low solid concentration, be that between two spheres of different species. The simultaneous interactions between three or more species of particle will be less common. This will also be the case for interactions between two particles of the same species in the absence of shear (there being zero relative velocity for such interacting particles). Thus, in this paper we make use of the linearity mentioned above to calculate the trajectories of two unlike solid spheres sedimenting in a stagnant flow and in a shear flow where one may have physical contact between the particles. Several methods have been used by others to calculate the hydrodynamic interactions between two spheres. These methods include the *method of reflections* (Happel & Brenner 1965), the use of *spherical bipolar coordinates* (Stimson & Jeffery 1926; Goldman *et al.* 1966; Lin *et al.* 1970), *twin multipole expansions* (Jeffrey & Onishi 1984) and the *collocation method* (Kim & Mifflin 1985). These methods in conjunction with lubrication theory have produced data which can be used for practical calculations of the trajectories of sedimenting particles. Among these methods we used those of Jeffrey & Onishi (1984) for particles sedimenting in a quiescent fluid and those of Kim & Mifflin (1985) for particles sedimenting in a shear flow.

2. STATEMENT AND FORMULATION OF THE PROBLEM

We consider two uniform solid spheres (labeled 1 and 2) having radii a_1 and a_2 and density ρ_1 and ρ_2, respectively, suspended in a Newtonian fluid of viscosity μ and density ρ. As shown in figure 1, we define at each instant of time a local system of coordinates (x, y, z) with the origin at the center of sphere number 1 and with the z axis directed along the line joining the sphere centers from sphere 1 to sphere 2. In this system the x–z plane is vertical and the y axis is horizontal. However, when we calculate the trajectories of the spheres we will use the fixed global system of coordinates (x', y', z') with the z' axis directed upwards. It will be assumed that as the spheres

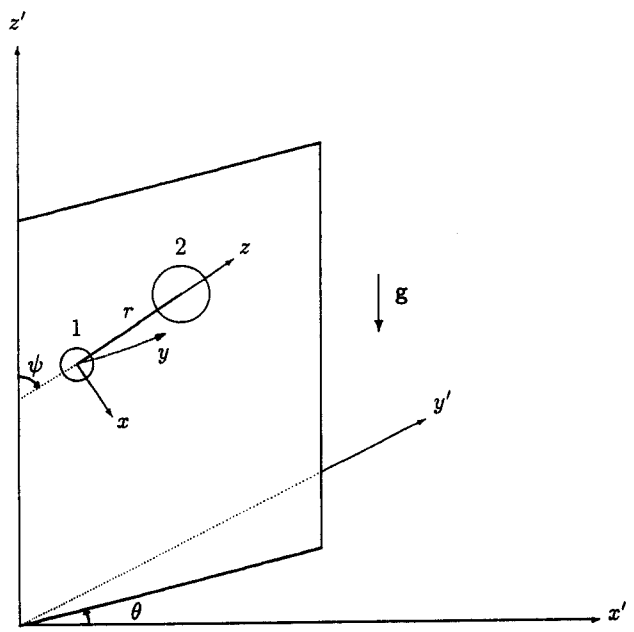

Figure 1. Illustration of two sedimenting spheres with the definition of the local (x, y, z) and global (x', y', z') systems of coordinates.

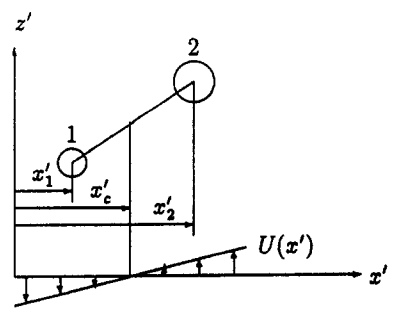

Figure 2. Definitions of the vertical component of the velocity field U for a positive value of γ and of the location of the center of the shear flow x'_c.

sediment they experience an undisturbed flow with velocity U, which is assumed to be the planar shear flow

$$\mathbf{U} = (0, 0, \gamma(x' - x'_c)), \tag{2}$$

with the velocity vertical and gradient in the horizontal x' direction. Here x'_c is the value of x' at the shear center (where the value of the velocity U is zero, see figure 2).

Since the Stokes equation [1] and the boundary conditions are linear, we may decompose the complex motion of spheres during their sedimentation into simpler motions. Consequently, the linear velocities ($\mathbf{V}^{(1)}$, $\mathbf{V}^{(2)}$) of the sphere centers and the angular velocities ($\mathbf{\Omega}^{(1)}$, $\mathbf{\Omega}^{(2)}$) of the spheres can be related to the forces ($\mathbf{F}^{(1)}$, $\mathbf{F}^{(2)}$) and the torques ($\mathbf{T}^{(1)}$, $\mathbf{T}^{(2)}$) about the sphere centers (applied to the fluid by the spheres) and to the rate of strain tensor E of the undisturbed velocity U through a grand mobility matrix, as follows:

$$\begin{bmatrix} \mathbf{V}^{(1)} \\ \mathbf{V}^{(2)} \\ \mathbf{\Omega}^{(1)} \\ \mathbf{\Omega}^{(2)} \end{bmatrix} = \mu^{-1} \begin{bmatrix} \mathbf{a}^{(11)} & \mathbf{a}^{(12)} & \mathbf{b}^{(11)} & \mathbf{b}^{(12)} & \mathbf{g}^{(1)} \\ \mathbf{a}^{(21)} & \mathbf{a}^{(22)} & \mathbf{b}^{(21)} & \mathbf{b}^{(22)} & \mathbf{g}^{(2)} \\ \mathbf{b}^{(11)} & \mathbf{b}^{(12)} & \mathbf{c}^{(11)} & \mathbf{c}^{(12)} & \mathbf{h}^{(1)} \\ \mathbf{b}^{(21)} & \mathbf{b}^{(22)} & \mathbf{c}^{(21)} & \mathbf{c}^{(22)} & \mathbf{h}^{(2)} \end{bmatrix} \begin{bmatrix} \mathbf{F}^{(1)} \\ \mathbf{F}^{(2)} \\ \mathbf{T}^{(1)} \\ \mathbf{T}^{(2)} \\ \mu\mathbf{E} \end{bmatrix} + \begin{bmatrix} \mathbf{U}_0^{(1)} \\ \mathbf{U}_0^{(2)} \\ \mathbf{\Omega}_0^{(1)} \\ \mathbf{\Omega}_0^{(2)} \end{bmatrix}, \tag{3}$$

where $E_{ij} = \frac{1}{2}(U_{i,j} + U_{j,i})$. The superscripts (1) and (2) used above refer to the sphere number, also $\mathbf{a}^{(\alpha\beta)}$, $\mathbf{b}^{(\alpha\beta)}$, $\tilde{\mathbf{b}}^{(\alpha\beta)}$ (transpose of $\mathbf{b}^{(\beta\alpha)}$) and $\mathbf{c}^{(\alpha\beta)}$ in [3] are second rank tensors and $\mathbf{g}^{(\alpha)}$ and $\mathbf{h}^{(\alpha)}$ are third rank tensors (Jeffrey & Onishi 1984; Kim & Mifflin 1985). In [3] $\mathbf{U}_0^{(\alpha)}$ and $\mathbf{\Omega}_0^{(\alpha)}$ are linear and angular velocity vectors (i.e. one half of the vorticity) of the undisturbed flow field evaluated at the location of the center of sphere α. The applied force $\mathbf{F}^{(\alpha)}$ exerted on the fluid by sphere α is the sum of the gravity and buoyancy forces exerted on the sphere if the inertia of the sphere is neglected. This can be written to the local system of coordinates (x, y, z) as follows:

$$\mathbf{F}^{(\alpha)} = (-F_g^{(\alpha)} \sin\psi, 0, F_g^{(\alpha)} \cos\psi), \quad (\alpha = 1, 2), \tag{4a}$$

where

$$F_g^{(\alpha)} = \frac{4\pi}{3}(\rho - \rho_\alpha) g a_\alpha^3 \tag{4b}$$

and g is the magnitude of the gravitational acceleration defined to be positive in the negative z' direction and ψ is the angle between the z' and z axes at any instant of motion (see figure 1). We assume that the spheres have a uniform mass distribution so that the applied torque on each sphere, and hence the torque $\mathbf{T}^{(\alpha)}$ that each sphere exerts on the fluid, is zero. Thus,

$$\mathbf{T}^{(\alpha)} = 0. \tag{5}$$

From [2] we have $\mathbf{U}_0^{(\alpha)}$, $\mathbf{\Omega}_0^{(\alpha)}$ and E relative to local system of coordinates as follows:

$$\mathbf{U}_0^{(\alpha)} = (-U^{(\alpha)} \sin\psi, 0, U^{(\alpha)} \cos\psi), \tag{6a}$$

$$\mathbf{\Omega}_0^{(\alpha)} = -\frac{\gamma}{2}(\cos\psi \sin\theta, \cos\theta, \sin\psi \sin\theta) \tag{6b}$$

and

$$\mathbf{E} = \frac{\gamma}{2} \begin{bmatrix} -\cos\theta \sin 2\psi & \sin\theta \sin\psi & \cos\theta \cos 2\psi \\ \sin\theta \sin\psi & 0 & -\sin\theta \cos\psi \\ \cos\theta \cos 2\psi & -\sin\theta \cos\psi & \cos\theta \sin 2\psi \end{bmatrix}, \tag{6c}$$

where $U^{(\alpha)} = (x'_\alpha - x'_c)\gamma$. We will refer all quantities in [3] to the local system of coordinates (x, y, z) in which the components of the mobility matrix are functions only of the sphere radii (a_1 and a_2) and the separation distance between the spheres' centers r (see figure 1). For the purpose of

performing the present calculation we used the results obtained by Jeffrey & Onishi (1984) for $\mathbf{a}^{(\alpha\beta)}$, $\mathbf{b}^{(\alpha\beta)}$, $\mathbf{\tilde{b}}^{(\alpha\beta)}$ and $\mathbf{c}^{(\alpha\beta)}$ (available for any value of the radius ratio $\lambda = a_2/a_1$, but not accurate when λ is very small or very large), and for the remaining elements we used the results obtained by Kim & Mifflin (1985) (available for only $\lambda = 1$). Once the mobility functions are known for a given position and given sizes of the spheres, we can calculate the velocity and angular velocity vectors of the spheres using [3] with the applied forces and torques given by [4a] and [5] and experiencing the shear flow field given by [2]. Then the trajectories of each sphere can be calculated numerically using an explicit scheme with respect to time t assuming a small time step δt. In these calculations the value of δt is taken to be proportional to r in order to have a larger time step when the spheres are far apart and the hydrodynamic interactions are weak. If during the motion, the gap between the spheres becomes equal to the surface roughness height ϵ, it is assumed that they will make physical contact. At this instant and during their subsequent motion while they are in contact we assume that the spheres lock together and do not slide on each other. In other words, they move as a rigid body (i.e. like a dumb-bell). This contact mode will continue until the component of the hydrodynamic force in the direction of the center-to-center line changes sign (and becomes repulsive). This occurs when the center-to-center line becomes horizontal (i.e. parallel to the x'–y' plane) since in this position this force component must be zero by symmetry. Then during their subsequent motion, the spheres separate and the interaction is again purely hydrodynamic. The following sections will present the details of calculations of trajectories of the two spheres sedimenting in a stagnant flow (i.e. pure sedimentation $\mathbf{U} = 0$), and also sedimenting in a shear flow ($\mathbf{U} \neq 0$). In order to do that it is convenient to use a dimensionless form of the variables. We follow Jeffrey & Onishi (1984) and define the dimensionless variables $\hat{\mathbf{a}}^{(\alpha\beta)}$, $\hat{\mathbf{b}}^{(\alpha\beta)}$ and $\hat{\mathbf{c}}^{(\alpha\beta)}$ as follows:

$$\hat{\mathbf{a}}^{(\alpha\beta)} = 3\pi(a_\alpha + a_\beta)\mathbf{a}^{(\alpha\beta)}, \quad [7a]$$

$$\hat{\mathbf{b}}^{(\alpha\beta)} = \pi(a_\alpha + a_\beta)^2\mathbf{b}^{(\alpha\beta)} \quad [7b]$$

and

$$\hat{\mathbf{c}}^{(\alpha\beta)} = \pi(a_\alpha + a_\beta)^3\mathbf{c}^{(\alpha\beta)}. \quad [7c]$$

We also define the dimensionless tensors $\hat{\mathbf{g}}^{(\alpha)}$ and $\hat{\mathbf{h}}^{(\alpha)}$ as follows:

$$\hat{\mathbf{g}}^{(\alpha)} = \frac{\mathbf{g}^{(\alpha)}}{(a_\alpha + a_{3-\alpha})} \quad [7d]$$

$$\hat{\mathbf{h}}^{(\alpha)} = \mathbf{h}^{(\alpha)}. \quad [7e]$$

For nondimensionalization of the linear and angular velocities, applied forces and torques and rate of strain tensor we define, respectively:

$$\hat{\mathbf{V}} = \frac{\mu\mathbf{V}}{g(\rho_1 - \rho)(a_1 + a_2)^2}, \quad [8a]$$

$$\hat{\mathbf{\Omega}} = \frac{\mu\mathbf{\Omega}}{g(\rho_1 - \rho)(a_1 + a_2)}, \quad [8b]$$

$$\hat{\mathbf{F}} = \frac{\mathbf{F}}{\pi g(\rho_1 - \rho)(a_1 + a_2)^3}, \quad [8c]$$

$$\hat{\mathbf{T}} = \frac{\mathbf{T}}{\pi g(\rho_1 - \rho)(a_1 + a_2)^4} \quad [8d]$$

and

$$\hat{\mathbf{E}} = \frac{\mu\mathbf{E}}{g(\rho_1 - \rho)(a_1 + a_2)}. \quad [8e]$$

By substituting [7a–e] and [8a–e] into [3], this equation can be written in terms of dimensionless variables as:

$$\begin{bmatrix} \hat{\mathbf{V}}^{(1)} \\ \hat{\mathbf{V}}^{(2)} \\ \hat{\boldsymbol{\Omega}}^{(1)} \\ \hat{\boldsymbol{\Omega}}^{(2)} \end{bmatrix} = \begin{bmatrix} \frac{(1+\lambda)}{6}\hat{\mathbf{a}}^{(11)} & \frac{1}{3}\hat{\mathbf{a}}^{(12)} & \frac{(1+\lambda)^2}{4}\hat{\mathbf{b}}^{(11)} & \hat{\mathbf{b}}^{(12)} & \hat{\mathbf{g}}^{(1)} \\ \frac{1}{3}\hat{\mathbf{a}}^{(21)} & \frac{\left(1+\frac{1}{\lambda}\right)}{6}\hat{\mathbf{a}}^{(22)} & \hat{\mathbf{b}}^{(21)} & \frac{\left(1+\frac{1}{\lambda}\right)^2}{4}\hat{\mathbf{b}}^{(22)} & \hat{\mathbf{g}}^{(2)} \\ \frac{(1+\lambda)^2}{4}\hat{\mathbf{b}}^{(11)} & \hat{\mathbf{b}}^{(12)} & \frac{(1+\lambda)^3}{8}\hat{\mathbf{c}}^{(11)} & \hat{\mathbf{c}}^{(12)} & \hat{\mathbf{h}}^{(1)} \\ \hat{\mathbf{b}}^{(21)} & \frac{\left(1+\frac{1}{\lambda}\right)^2}{4}\hat{\mathbf{b}}^{(22)} & \hat{\mathbf{c}}^{(21)} & \frac{\left(1+\frac{1}{\lambda}\right)^3}{8}\hat{\mathbf{c}}^{(22)} & \hat{\mathbf{h}}^{(2)} \end{bmatrix} \begin{bmatrix} \hat{\mathbf{F}}^{(1)} \\ \hat{\mathbf{F}}^{(2)} \\ \hat{\mathbf{T}}^{(1)} \\ \hat{\mathbf{T}}^{(2)} \\ \hat{\mathbf{E}} \end{bmatrix} + \begin{bmatrix} \hat{\mathbf{U}}_0^{(1)} \\ \hat{\mathbf{U}}_0^{(2)} \\ \hat{\boldsymbol{\Omega}}_0^{(1)} \\ \hat{\boldsymbol{\Omega}}_0^{(2)} \end{bmatrix}. \quad [9]$$

In what follows all lengths are made dimensionless with the quantity $a_1 + a_2$ while t and shear rate γ are made dimensionless as follows:

$$\hat{t} = \frac{g|\rho_1 - \rho|(a_1 + a_2)t}{\mu} \quad [10a]$$

and

$$\hat{\gamma} = \frac{\mu\gamma}{g(\rho_1 - \rho)(a_1 + a_2)}. \quad [10b]$$

The tensors $\hat{\mathbf{a}}^{(\alpha\beta)}$, $\hat{\mathbf{b}}^{(\alpha\beta)}$, $\hat{\mathbf{c}}^{(\alpha\beta)}$, $\hat{\mathbf{g}}^{(\alpha)}$ and $\hat{\mathbf{h}}^{(\alpha)}$ are then functions only of the radius ratio λ and the dimensionless distance between the sphere centers $\hat{r} = r/(a_1 + a_2)$.

3. PURE SEDIMENTATION ($\mathbf{U} = 0$)

In this section we will give the details of the calculation of the trajectories of two spheres of arbitrary sizes and densities sedimenting in a quiescent fluid ($\mathbf{U} = 0$). It can be shown by symmetry that such trajectories must lie in a fixed vertical plane which we may take, without loss of generality, to be the x'–z' plane, so that $\theta = 0$ throughout the motion (see figure 1).

We will consider two possible cases. For case 1, we will assume that the spheres are ideally smooth and the interactions are purely hydrodynamic (i.e. spheres do not make physical contact). For case 2, we let the spheres make physical contact if their gap width becomes equal to their dimensional roughness height ϵ. In order to find the trajectories of the two spheres we use [9] with $\hat{\mathbf{E}} = 0$, $\hat{\mathbf{U}}_0^{(\alpha)} = 0$, $\hat{\boldsymbol{\Omega}}_0^{(\alpha)} = 0$ and $\hat{\mathbf{F}}^{(\alpha)}$ and $\hat{\mathbf{T}}^{(\alpha)}$ given by [4a] and [5] and made nondimensional by [8a–e]. Therefore, we do not need to calculate the tensors $\hat{\mathbf{g}}^{(\alpha)}$ and $\hat{\mathbf{h}}^{(\alpha)}$. It is, however, necessary to calculate all other elements of the mobility matrix in [9]. These elements are functions only of λ and $\hat{r}$ and are calculated using the results obtained by Jeffrey & Onishi (1984). The calculated linear and angular velocities obtained from [9] are then transformed to the global system of coordinates (x', y', z') using

$$\begin{bmatrix} \hat{V}_{x'}^{(\alpha)} \\ V_{y'}^{(\alpha)} \\ \hat{V}_{z'}^{(\alpha)} \end{bmatrix} = \begin{bmatrix} \cos\psi & 0 & \sin\psi \\ 0 & 1 & 0 \\ -\sin\psi & 0 & \cos\psi \end{bmatrix} \begin{bmatrix} \hat{V}_x^{(\alpha)} \\ \hat{V}_y^{(\alpha)} \\ \hat{V}_z^{(\alpha)} \end{bmatrix} \quad [11]$$

with a similar equation for $\hat{\boldsymbol{\Omega}}^{(\alpha)}$. Therefore, knowing the positions of the spheres at any time t (i.e. the values of $\hat{r}$ and ψ), we can calculate numerically their displacements at time $t + \delta t$ by multiplying δt by the linear velocities of the spheres. Then, knowing the new positions of the spheres (i.e. new values of $\hat{r}$ and ψ), we can calculate the new mobility matrix and applied forces and torques and consequently repeat the calculations in the same manner in order to obtain the paths of the

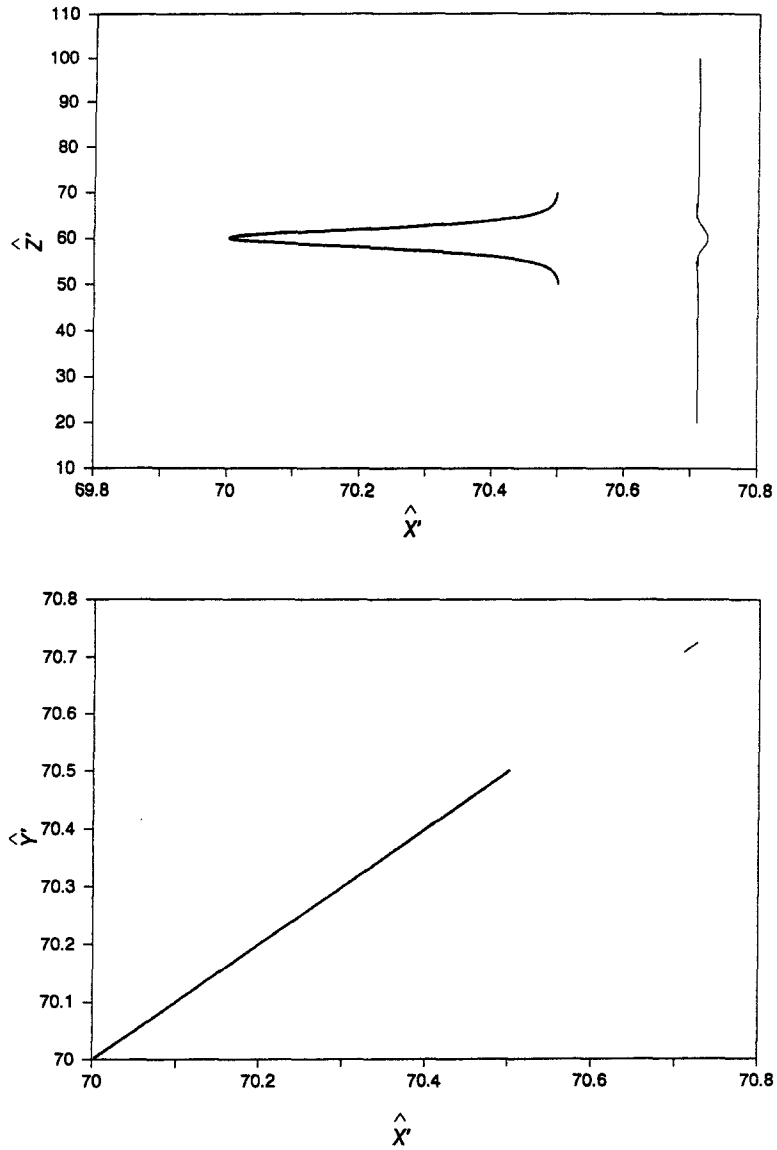

Figure 3. Trajectories of two ideally smooth unequal spheres ($\lambda = 2$ and $\kappa = 4$; thick lines represent sphere 1 and thin lines represent sphere 2) sedimenting in a quiescent fluid without making contact. Initial values of $\hat{r}$, ψ and θ are 30, 0.573° and 45°, respectively. $\hat{x}' = x'/(a_1 + a_2)$ etc.

spheres. Typical results are shown in figure 3 for two interacting spheres with a large initial separation in the z' direction. This demonstrates the symmetry of the trajectories about a horizontal plane and zero net displacements of the spheres in the x' direction (a result which follows directly from the linearity of the equations and boundary conditions) as well as zero displacement out of the vertical plane of sedimentation (which follows from the symmetry of the problem when $\mathbf{U} = 0$). It is worth noting that λ and the relative density κ [$\kappa = (\rho_2 - \rho)/(\rho_1 - 1)$] must satisfy $\lambda^2\kappa \neq 1$ in order to have a nonzero relative velocity for the sedimenting spheres at large separation distances.

For case 2, in which contact between the spheres may occur, we assume that the surfaces of the spheres have a typical dimensionless roughness equal to $\hat{\epsilon}$ [$\hat{\epsilon} = \epsilon/(a_1 + a_2)$] which is normally very small compared to unity. Then during the sedimentation process when the dimensionless gap $\hat{r} - 1$ between the spheres becomes equal to $\hat{\epsilon}$ as a result of their hydrodynamic interactions, contact will occur. We suppose this occurs when ψ has the value ψ^*. In order to analyze the rigid-body motion of the spheres in contact we suppose the spheres are joined by a rod of negligible cross section with dimensional length l_r which will be taken to be equal to ϵ, and is hence small compared with the

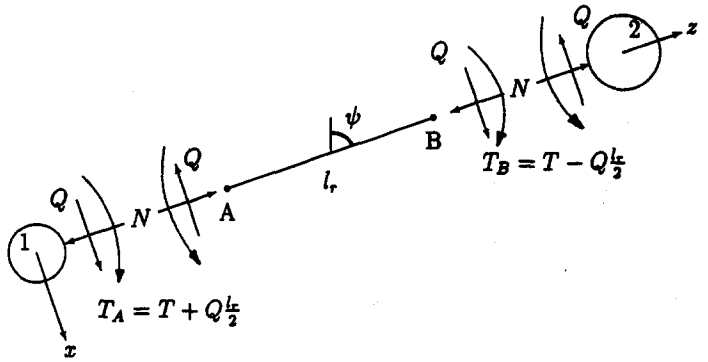

Figure 4. Free-body diagrams of two spheres and of a rod joining them, while sedimenting in a Stokes flow.

sphere radii. However, the rigid-body motion of the dumb-bell which will be obtained is not restricted to these small values of l_r. In fact l_r can take any positive value as long as the cross section of the rod is sufficiently small so that the hydrodynamic forces and torques on the rod itself can be neglected.

Considering the free-body diagram of the imaginary rod of length l_r (see figure 4), if at end A, the forces on the rod along and perpendicular to the rod are N and Q, then those at the other end B are equal in magnitude and opposite in direction as shown. The applied torques T_A and T_B acting on the rod at A and B, respectively, are then related by

$$T_B = T_A - Ql_r.$$

For the purpose of simplifying the algebra, we let $T_A = T + (l_r/2)Q$ so that $T_B = T - (l_r/2)Q$. By applying the conditions of equilibrium for sphere 1 it is seen that the hydrodynamic force and torque (about the center of sphere 1) exerted on the fluid by this sphere is (relative to the local x, y, z coordinates), when expressed in terms of dimensionless quantities (see [8a–e]):

$$\hat{\mathbf{F}}^{(1)} = (-\hat{F}_g^{(1)} \sin\psi + \hat{Q}, 0, \hat{F}_g^{(1)} \cos\psi - \hat{N}) \qquad [12a]$$

and

$$\hat{\mathbf{T}}^{(1)} = \left(0, \hat{T} + \frac{1}{2}\left(\frac{1-\lambda}{1+\lambda} + \hat{r}\right)\hat{Q}, 0\right), \qquad [12b]$$

where $\hat{Q}$, $\hat{N}$ and $\hat{T}$ are, respectively, the dimensionless forms of Q, N and T (see [8a–e]) and where

$$\hat{F}_g^{(1)} = -\frac{4}{3(1+\lambda)^3}.$$

Similarly, the hydrodynamic forces and torques (about the center of sphere 2) exerted on the fluid by sphere 2 are:

$$\hat{\mathbf{F}}^{(2)} = (-\hat{F}_g^{(2)} \sin\psi - \hat{Q}, 0, \hat{F}_g^{(2)} \cos\psi + \hat{N}) \qquad [13a]$$

and

$$\hat{\mathbf{T}}^{(2)} = \left(0, -\hat{T} - \frac{1}{2}\left(\frac{1-\lambda}{1+\lambda} - \hat{r}\right)\hat{Q}, 0\right), \qquad [13b]$$

where

$$\hat{\mathbf{F}}_g^{(2)} = -\frac{4\kappa}{3\left(1+\frac{1}{\lambda}\right)^3}.$$

If these values are substituted into [9], which now takes the form

$$\hat{\mathbf{V}}^{(1)} = \frac{1+\lambda}{6}\hat{\mathbf{a}}^{(11)}\hat{\mathbf{F}}^{(1)} + \tfrac{1}{3}\hat{\mathbf{a}}^{(12)}\hat{\mathbf{F}}^{(2)} + \frac{(1+\lambda)^2}{4}\hat{\mathbf{b}}^{(11)}\hat{\mathbf{T}}^{(1)} + \hat{\mathbf{b}}^{(12)}\hat{\mathbf{T}}^{(2)}, \tag{14a}$$

$$\hat{\mathbf{V}}^{(2)} = \tfrac{1}{3}\hat{\mathbf{a}}^{(21)}\hat{\mathbf{F}}^{(1)} + \frac{\left(1+\frac{1}{\lambda}\right)}{6}\hat{\mathbf{a}}^{(22)}\hat{\mathbf{F}}^{(2)} + \hat{\mathbf{b}}^{(21)}\hat{\mathbf{T}}^{(1)} + \frac{\left(1+\frac{1}{\lambda}\right)^2}{4}\hat{\mathbf{b}}^{(22)}\hat{\mathbf{T}}^{(2)}, \tag{14b}$$

$$\hat{\boldsymbol{\Omega}}^{(1)} = \frac{(1+\lambda)^2}{4}\hat{\mathbf{b}}^{(11)}\hat{F}^{(1)} + \hat{\mathbf{b}}^{(12)}\hat{\mathbf{F}}^{(2)} + \frac{(1+\lambda)^3}{8}\hat{\mathbf{c}}^{(11)}\hat{\mathbf{T}}^{(1)} + \hat{\mathbf{c}}^{(12)}\hat{\mathbf{T}}^{(2)} \tag{14c}$$

and

$$\hat{\boldsymbol{\Omega}}^{(2)} = \hat{\mathbf{b}}^{(21)}\hat{\mathbf{F}}^{(1)} + \frac{\left(1+\frac{1}{\lambda}\right)^2}{4}\hat{\mathbf{b}}^{(22)}\hat{\mathbf{F}}^{(2)} + \hat{\mathbf{c}}^{(21)}\hat{\mathbf{T}}^{(1)} + \frac{\left(1+\frac{1}{\lambda}\right)^3}{8}\hat{\mathbf{c}}^{(22)}\hat{\mathbf{T}}^{(2)}, \tag{14d}$$

we obtain 12 scalar equations involving 15 unknowns. Twelve of these unknowns are the components of $\hat{\mathbf{V}}^{(\alpha)}$ and $\hat{\boldsymbol{\Omega}}^{(\alpha)}$ with the remaining being $\hat{Q}$, $\hat{N}$ and $\hat{T}$. Therefore, we need three more equations. These equations are supplied using the kinematic constraints resulting from the assumption of rigid-body motion of the dumb-bell consisting of the two spheres and rod. These constraints are

$$\hat{\Omega}_y^{(1)} = \hat{\Omega}_y^{(2)} \quad (=\hat{\Omega}; \text{ say}), \tag{15a}$$

$$\hat{V}_x^{(2)} = \hat{V}_x^{(1)} + \hat{\Omega}\hat{r} \tag{15b}$$

and

$$\hat{V}_z^{(1)} = \hat{V}_z^{(2)}. \tag{15c}$$

Hence by solving [14a–d] and [15a–c] we obtain the 15 unknowns as follows:

$$\hat{T} = K_T \sin\psi, \quad \hat{Q} = K_Q \sin\psi, \quad \hat{N} = K_N \cos\psi, \quad \hat{V}_x^{(1)} = B_1 \sin\psi, \tag{16a–d}$$

$$\hat{V}_z^{(1)} = C_1 \cos\psi, \quad \hat{V}_y^{(1)} = \hat{\Omega}_x^{(1)} = \hat{\Omega}_z^{(1)} = 0, \quad \hat{V}_x^{(2)} = B_2 \sin\psi \tag{16e–g}$$

$$\hat{V}_z^{(2)} = C_1 \cos\psi, \quad \hat{V}_y^{(2)} = \hat{\Omega}_x^{(2)} = \hat{\Omega}_z^{(2)} = 0, \quad \hat{\Omega}_y^{(1)} = \hat{\Omega}_y^{(2)} = A \sin\psi, \tag{16h–j}$$

where all coefficients are functions of $\hat{F}_g^{(\alpha)}$, $\hat{r}$ and λ (see appendix A). Now we transfer the linear and angular velocities to the global system of coordinates using [11] to obtain

$$\hat{V}_{x'}^{(\alpha)} = (B_\alpha + C_\alpha)\sin\psi\cos\psi, \tag{17a}$$

$$\hat{V}_{z'}^{(\alpha)} = -(B_\alpha + C_\alpha)\sin^2\psi + C_\alpha \tag{17b}$$

and

$$\hat{\Omega}_{y'}^{(\alpha)} = A \sin\psi. \tag{17c}$$

The dimensionless values of the coordinates of the centers of the spheres ($\hat{x}'_\alpha$ and $\hat{z}'_\alpha$) and the angle ψ are related to the velocities and angular velocities of the spheres by

$$\frac{\mathrm{d}\hat{x}'_\alpha}{\mathrm{d}\hat{t}} = \mathrm{sgn}(\rho_1 - \rho)\hat{V}_{x'}^{(\alpha)}, \tag{18a}$$

$$\frac{\mathrm{d}\hat{z}'_\alpha}{\mathrm{d}\hat{t}} = \mathrm{sgn}(\rho_1 - \rho)\hat{V}_{z'}^{(\alpha)} \tag{18b}$$

and

$$\frac{\mathrm{d}\psi}{\mathrm{d}\hat{t}} = \mathrm{sgn}(\rho_1 - \rho)\hat{\Omega}. \tag{18c}$$

By dividing [18a] and [18b] by [18c] we obtain, respectively,

$$\frac{d\hat{x}'_\alpha}{d\psi} = \frac{B_\alpha + C_\alpha}{A} \cos\psi \qquad [19a]$$

and

$$\frac{d\hat{z}'_\alpha}{d\psi} = -\frac{B_\alpha + C_\alpha}{A} \sin\psi + \frac{C_\alpha}{A \sin\psi}; \qquad [19b]$$

which may be integrated to give

$$\hat{x}'_\alpha = \frac{B_\alpha + C_\alpha}{A} (\sin\psi - \sin\psi^*) + \hat{x}'^*_\alpha \qquad [20a]$$

and

$$\hat{z}'_\alpha = \frac{B_\alpha + C_\alpha}{A} (\cos\psi - \cos\psi^*) + \frac{C_\alpha}{A} \left[\ln \frac{\tan(\psi/2)}{\tan(\psi^*/2)} \right] + \hat{z}'^*_\alpha, \qquad [20b]$$

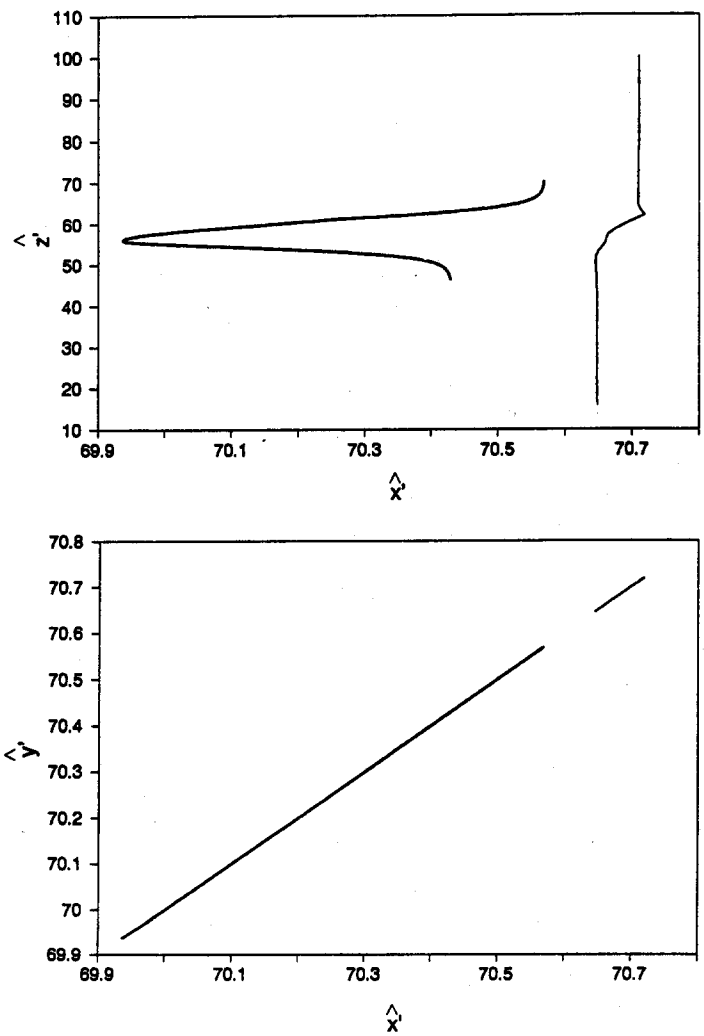

Figure 5. Trajectories of two unequal spheres ($\lambda = 2$ and $\kappa = 4$; thick lines represent sphere 1 and thin lines represent sphere 2) sedimenting in a quiescent fluid and making contact ($\hat{\epsilon} = 0.025$). Initial values of $\hat{r}$, ψ and θ are 30, 0.382° and 45°, respectively.

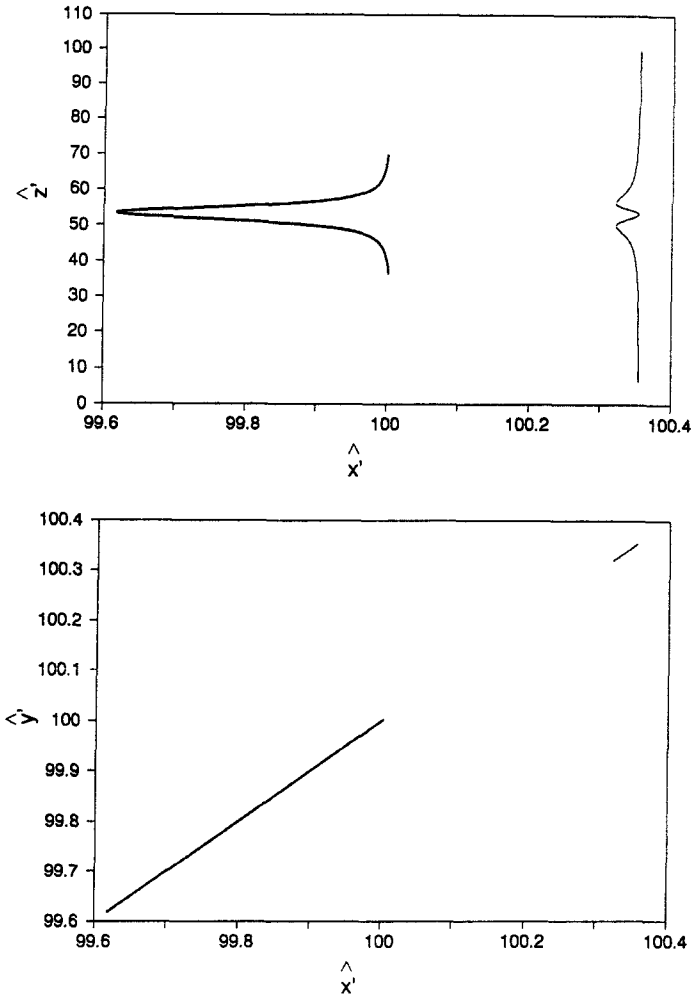

Figure 6. Trajectories of two equal spheres ($\lambda = 1$ and $\kappa = 4$) sedimenting in a shear flow with $\hat{\gamma} = -0.05$ without making contact; initial values of $\hat{r}$, ψ and θ are 30, 0.573° and 45°, respectively.

where, ψ^*, $\hat{x}_\alpha'^*$ and $\hat{z}_\alpha'^*$ are the values of ψ, $\hat{x}_\alpha'$ and $\hat{z}_\alpha'$, respectively, at the instant when the contact begins. Also, integration of [18c] yields

$$\tan\left(\frac{\psi}{2}\right) = \tan\left(\frac{\psi^*}{2}\right) e^{[A\,\mathrm{sgn}(\rho_1 - \rho)t]}. \qquad [20c]$$

Equations [20a, b] describe parametrically the trajectories of the two spheres in contact. The complete trajectories are obtained by using a computer program which calculates the trajectories of the spheres while they are not in contact, as described for case 1, and when they are in contact by making use of [20a, b]. Contact occurs at the instant when the dimensionless gap $\hat{r} - 1$ is equal to $\hat{\epsilon}$ and continues until the line joining the centers becomes horizontal (see section 2). We observe that the trajectories (see figure 5) of the spheres in the x'–z' plane are, unlike the case of no contact, no longer symmetrical about any horizontal plane. In addition, there is a net horizontal displacement of the spheres as a result of their mutual interaction. These "nonlinear" effects are due to the physical contact of the spheres in the course of their sedimentation.

4. SEDIMENTATION IN SHEAR FLOW ($\mathbf{U} \neq 0$)

In this section we consider again the problem of two sedimenting spheres but now include the effect of a superimposed velocity field $\mathbf{U}$ given by [2]. The motion of the spheres, unlike that for the case of pure sedimentation, is three-dimensional with their trajectories depending on the initial

value of the polar angle θ (see figure 1). The x', y', z' axes were taken in such a manner as to make $x' = x'_c$ (see [2]) at the mid-point between the spheres at the start of the calculation. A different choice for the point $x' = x'_c$ would merely result in a constant vertical velocity being added to the spheres' motion.

In order to analyze the problem of the sedimentation of two spheres in a shear flow, we again consider two cases. For case 1, we will calculate the trajectories of the spheres sedimenting in a shear flow when no contact occurs between the spheres. For case 2, the trajectories of the spheres will be obtained when physical contact occurs between the spheres. In order to calculate the paths of the centers of the spheres we again make use of [9] in which $\hat{\mathbf{U}}_0^{(\alpha)}$, $\hat{\boldsymbol{\Omega}}_0^{(\alpha)}$ and $\hat{\mathbf{E}}$ are given by [6a–c] and $\hat{\mathbf{F}}^{(\alpha)}$ and $\hat{\mathbf{T}}^{(\alpha)}$ are given by [4a] and [5] and made nondimensional by [8a–e]. Since the rate of strain tensor is not zero we have to calculate the dimensionless mobility tensors $\hat{\mathbf{g}}^{(\alpha)}$ and $\hat{\mathbf{h}}^{(\alpha)}$. Like the other elements of the mobility matrix, the elements of these tensors are functions of $\hat{r}$ and λ. However, the complete results [obtained by Kim & Mifflin (1985)] are available for only $\lambda = 1$ and $\hat{r} \geqslant 1.01$. Therefore, we restrict our calculations for two equal-size spheres with differing densities. Typical results obtained for case 1 are shown in figure 6 which demonstrates the symmetry of the trajectories about a horizontal plane as well as zero net displacement in the x' direction. For case 2, in which we assume that the spheres make physical contact when their gap (i.e. $\hat{r} - 1$) becomes equal to their dimensionless surface roughness height $\hat{\epsilon}$, we suppose contact occurs when ψ and θ have the values ψ^* and θ^* and that from this position on, the spheres are locked together and undergo rigid-body motion until $\psi = \pi/2$ when the spheres separate and continue their purely hydrodynamic motion. In order to analyze the motion of this dumb-bell-type body formed when the spheres are locked together we will follow essentially the same approach as we did for the pure sedimentation case, except that in this case we must take into account the three-dimensional motion of the spheres. For this purpose we again consider the free-body diagrams of the spheres and a rod with negligible cross section joining them, as shown in figure 7. First we consider the free-body diagram of the rod having length l_r. In the local system of coordinates and in the x–z plane

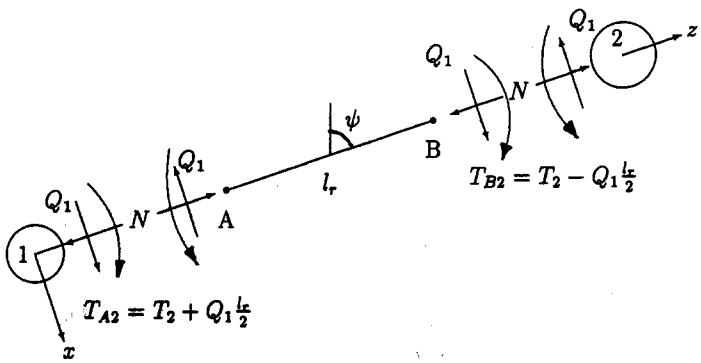

(a)

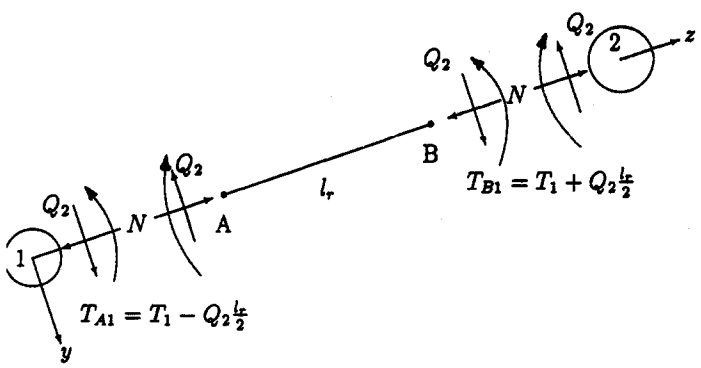

(b)

Figure 7. Free-body diagrams of two spheres and of an imaginary rod joining them: (a) projection on the x–z plane; and (b) projection on the y–z plane.

[see figure 7(a)] the mechanical shear force $-Q_1$, the normal force N and the mechanical torque T_{A2}, act at end A of the rod. By writing the equation of equilibrium for the rod we find that the applied forces at the end B of the rod are Q_1 and $-N$ and the applied torque T_{B2}, where

$$T_{B2} = T_{A2} - Q_1 l_r.$$

For the purpose of simplifying the algebra we let $T_{A2} = T_2 + (l_r/2)Q_1$, so that $T_{B2} = T_2 - (l_r/2)Q_1$. Likewise, for equilibrium in the y–z plane we have the situation shown in figure 7(b), in which $T_{A1} = T_1 - (l_r/2)Q_2$ and $T_{B1} = T_1 + (l_r/2)Q_2$. By applying the condition of equilibrium for sphere 1, it is seen that the hydrodynamic force and torque (about the center of the sphere 1) acting on the fluid by this sphere (for $\lambda = 1$) are (relative to the local system of coordinates), when expressed in terms of dimensionless quantities (see [8a–e]):

$$\hat{\mathbf{F}}^{(1)} = (-\hat{F}_g^{(1)} \sin\psi + \hat{Q}_1, \hat{Q}_2, \hat{F}_g^{(1)} \cos\psi - \hat{N}) \tag{21a}$$

and

$$\hat{\mathbf{T}}^{(1)} = \left(\hat{T}_1 - \frac{\hat{r}}{2}\hat{Q}_2, \hat{T}_2 + \frac{\hat{r}}{2}\hat{Q}_1, 0\right). \tag{21b}$$

Similarly, the hydrodynamic forces and torques (about the center of sphere 2) on the fluid by sphere 2 must be

$$\hat{\mathbf{F}}^{(2)} = (-\hat{F}_g^{(2)} \sin\psi - \hat{Q}_1, -\hat{Q}_2, \hat{F}_g^{(2)} \cos\psi + \hat{N}) \tag{22a}$$

and

$$\hat{\mathbf{T}}^{(2)} = \left(-\hat{T}_1 - \frac{\hat{r}}{2}\hat{Q}_2, -\hat{T}_2 + \frac{\hat{r}}{2}\hat{Q}_1, 0\right). \tag{22b}$$

If these values are substituted into [9], which now takes the form

$$\hat{\mathbf{V}}^{(1)} = \frac{\hat{\mathbf{a}}^{(11)}}{3}\hat{\mathbf{F}}^{(1)} + \frac{\hat{\mathbf{a}}^{(12)}}{3}\hat{\mathbf{F}}^{(2)} + \hat{\mathbf{b}}^{(11)}\hat{\mathbf{T}}^{(1)} + \hat{\mathbf{b}}^{(12)}\hat{\mathbf{T}}^{(2)} + \hat{\mathbf{g}}^{(1)}\hat{\mathbf{E}} + \hat{\mathbf{U}}_0^{(1)}, \tag{23a}$$

$$\hat{\mathbf{V}}^{(2)} = \frac{\hat{\mathbf{a}}^{(21)}}{3}\hat{\mathbf{F}}^{(1)} + \frac{\hat{\mathbf{a}}^{(22)}}{3}\hat{\mathbf{F}}^{(2)} + \hat{\mathbf{b}}^{(21)}\hat{\mathbf{T}}^{(1)} + \hat{\mathbf{b}}^{(22)}\hat{\mathbf{T}}^{(2)} + \hat{\mathbf{g}}^{(2)}\hat{\mathbf{E}} + \hat{\mathbf{U}}_0^{(2)}, \tag{23b}$$

$$\hat{\mathbf{\Omega}}^{(1)} = \hat{\mathbf{b}}^{(11)}\hat{\mathbf{F}}^{(1)} + \hat{\mathbf{b}}^{(12)}\hat{\mathbf{F}}^{(2)} + \hat{\mathbf{c}}^{(11)}\hat{\mathbf{T}}^{(1)} + \hat{\mathbf{c}}^{(12)}\hat{\mathbf{T}}^{(2)} + \hat{\mathbf{h}}^{(1)}\hat{\mathbf{E}} + \hat{\mathbf{\Omega}}_0^{(1)} \tag{23c}$$

and

$$\hat{\mathbf{\Omega}}^{(2)} = \hat{\mathbf{b}}^{(21)}\hat{\mathbf{F}}^{(1)} + \hat{\mathbf{b}}^{(22)}\hat{\mathbf{F}}^{(2)} + \hat{\mathbf{c}}^{(21)}\hat{\mathbf{T}}^{(1)} + \hat{\mathbf{c}}^{(22)}\hat{\mathbf{T}}^{(2)} + \hat{\mathbf{h}}^{(2)}\hat{\mathbf{E}} + \hat{\mathbf{\Omega}}_0^{(2)}, \tag{23d}$$

we have 12 scalar equations and 17 unknowns. Twelve of these unknowns are the components of $\hat{\mathbf{V}}^{(\alpha)}$ and $\hat{\mathbf{\Omega}}^{(\alpha)}$ and five of them are $\hat{T}_1$, $\hat{T}_2$, $\hat{Q}_1$, $\hat{Q}_2$ and $\hat{N}$. Therefore we need five more equations to have a determined system of equations. Again we invoke the consequences of rigid-body motion of the spheres in contact to obtain the required additional equations:

$$\hat{V}_z^{(1)} = \hat{V}_z^{(2)}, \quad \hat{V}_x^{(2)} = \hat{V}_x^{(1)} + \hat{\Omega}_y^{(1)}\hat{r}, \quad \hat{V}_y^{(2)} = \hat{V}_y^{(1)} - \hat{\Omega}_x^{(1)}\hat{r}, \tag{24a–c}$$

$$\hat{\Omega}_x^{(1)} = \hat{\Omega}_x^{(2)} \quad (=\hat{\Omega}_x; \text{ say}), \quad \hat{\Omega}_y^{(1)} = \hat{\Omega}_y^{(2)} (=\hat{\Omega}_y; \text{ say}). \tag{24d, e}$$

We can now solve equations [23a–d] and [24a–e] to obtain

$$\hat{T}_1 = 0, \tag{25a}$$

$$\hat{T}_2 = K_{T2} \sin\psi, \tag{25b}$$

$$\hat{Q}_1 = K_1 \sin\psi + K_2 \cos\theta \cos 2\psi + K_3 \cos\theta, \tag{25c}$$

$$\hat{Q}_2 = K_4 \sin\theta \cos\psi, \tag{25d}$$

$$\hat{N} = K_5 \cos\psi + K_6 \cos\theta \sin 2\psi, \tag{25e}$$

$$\hat{V}_x^{(1)} = E_1^{(1)} \sin\psi + E_2^{(1)} \cos\theta \cos 2\psi + E_3^{(1)} \cos\theta, \quad [25f]$$

$$\hat{V}_y^{(1)} = F_1 \sin\theta \cos\psi, \quad [25g]$$

$$\hat{V}_z^{(1)} = G_1^{(1)} \cos\psi + G_2^{(1)} \cos\theta \sin 2\psi, \quad [25h]$$

$$\hat{\Omega}_y^{(1)} = \hat{\Omega}_y^{(2)} = H_1 \sin\psi + H_2 \cos\theta \cos 2\psi + H_3 \cos\theta, \quad [25i]$$

$$\hat{\Omega}_x^{(1)} = \hat{\Omega}_x^{(2)} = L_1 \sin\theta \cos\psi, \quad [25j]$$

$$\hat{V}_x^{(2)} = E_1^{(2)} \sin\psi + E_2^{(2)} \cos\theta \cos 2\psi + E_3^{(2)} \cos\theta, \quad [25k]$$

$$\hat{V}_y^{(2)} = F_2 \sin\theta \cos\psi, \quad [25l]$$

$$\hat{V}_z^{(2)} = G_1^{(2)} \cos\psi + G_2^{(2)} \cos\theta \sin 2\psi \quad [25m]$$

and

$$\hat{\Omega}_z^{(1)} = \hat{\Omega}_z^{(2)} = 0, \quad [25n]$$

where all coefficients are functions of $\hat{F}_g^{(\alpha)}$, $\hat{y}$, λ and $\hat{r}$ (see appendix B). The linear and angular velocities of the spheres written relative to the global system (x', y', z') are

$$\hat{V}_{x'}^{(\alpha)} = \hat{V}_x^{(\alpha)} \cos\psi \cos\theta - \hat{V}_y^{(\alpha)} \sin\theta + \hat{V}_z^{(\alpha)} \sin\psi \cos\theta, \quad [26a]$$

$$\hat{V}_{y'}^{(\alpha)} = \hat{V}_x^{(\alpha)} \cos\psi \sin\theta + \hat{V}_y^{(\alpha)} \cos\theta + \hat{V}_z^{(\alpha)} \sin\psi \sin\theta, \quad [26b]$$

$$\hat{V}_{z'}^{(\alpha)} = -\hat{V}_x^{(\alpha)} \sin\psi + \hat{V}_z^{(\alpha)} \cos\theta, \quad [26c]$$

$$\hat{\Omega}_{x'}^{(\alpha)} = \hat{\Omega}_x \cos\psi \cos\theta - \hat{\Omega}_y \sin\theta, \quad [26d]$$

$$\hat{\Omega}_{y'}^{(\alpha)} = \hat{\Omega}_x \cos\psi \sin\theta + \hat{\Omega}_y \cos\theta \quad [26e]$$

and

$$\hat{\Omega}_{z'}^{(\alpha)} = -\hat{\Omega}_x \sin\psi. \quad [26f]$$

In order to obtain the trajectories of the spheres' centers we should therefore integrate the following relations with respect to time:

$$\frac{d\hat{x}'_\alpha}{d\hat{t}} = \mathrm{sgn}(\rho_1 - \rho)\hat{V}_{x'}^{(\alpha)}, \quad [27a]$$

$$\frac{d\hat{y}'_\alpha}{d\hat{t}} = \mathrm{sgn}(\rho_1 - \rho)\hat{V}_{y'}^{(\alpha)}, \quad [27b]$$

$$\frac{d\hat{z}'_\alpha}{d\hat{t}} = \mathrm{sgn}(\rho_1 - \rho)\hat{V}_{z'}^{(\alpha)}, \quad [27c]$$

$$\frac{d\psi}{d\hat{t}} = \mathrm{sgn}(\rho_1 - \rho)\hat{\Omega}_y \quad [27d]$$

and

$$\frac{d\theta}{d\hat{t}} = -\mathrm{sgn}(\rho_1 - \rho)\frac{\hat{\Omega}_x}{\sin\psi}. \quad [27e]$$

By eliminating the time variable $\hat{t}$ from the above relations we get

$$\frac{d\theta}{d\psi} = -\frac{\hat{\Omega}_x}{\hat{\Omega}_y \sin\psi}, \quad [28a]$$

$$\frac{d\hat{x}'_\alpha}{d\psi} = \frac{\hat{V}_{x'}^{(\alpha)}}{\hat{\Omega}_y}, \quad [28b]$$

$$\frac{d\hat{y}'_\alpha}{d\psi} = \frac{\hat{V}_{y'}^{(\alpha)}}{\hat{\Omega}_y} \quad [28c]$$

and

$$\frac{d\hat{z}'_\alpha}{d\psi} = \frac{\hat{V}_{z'}^{(\alpha)}}{\hat{\Omega}_y}. \qquad [28d]$$

Unlike the case of the pure sedimentation for which the equations determining the motion ([19a, b]) can be solved analytically, this cannot be done for the present case. Instead, we must integrate the system of five coupled ordinary differential equations given by [27a–e] numerically, using a forward explicit scheme in time.

The complete trajectories of spheres, while they are not in contact and when they are in contact are calculated by using a computer program based on the analysis presented in this section. This program calculates the trajectories of equal-size spheres with different densities sedimenting in a shear flow field. Typical results of calculated trajectories are shown in figure 8. As for the case of sedimentation alone, the trajectories of the spheres are not symmetrical about any horizontal plane and the spheres have net displacements in the $\hat{x}'$ and $\hat{y}'$ directions. However, unlike the case of sedimentation alone, the trajectories are no longer planar with their projections on the x'–y' plane no longer being straight lines.

Since it has been shown here that rough spheres experience net horizontal displacement $\Delta\hat{x}'_\alpha$ ($\alpha = 1, 2$) as a result of their physical contact, it seems of value to investigate the variation of $\Delta\hat{x}'_\alpha$ vs the spheres' surface roughness height. For this purpose we chose the same pair of spheres whose trajectories are shown in figure 8 (i.e. $\lambda = 1$, $\kappa = 4$ and $\hat{\gamma} = -0.05$) and calculated their net displacements in the x' direction for different values of $\hat{\epsilon}$. The results obtained are shown in

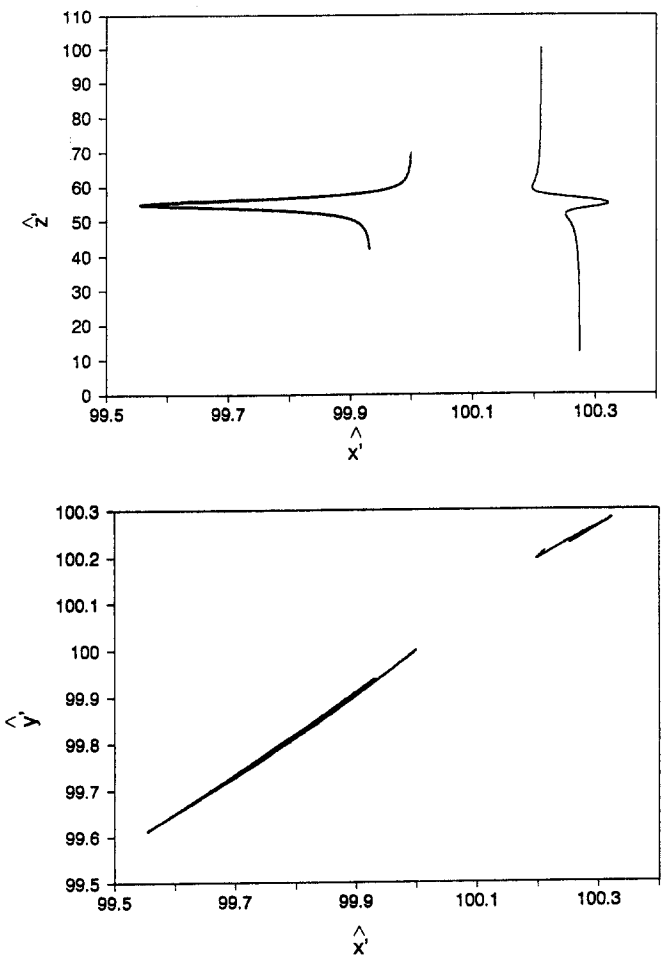

Figure 8. Trajectories of two equal spheres ($\lambda = 1$ and $\kappa = 4$; thick lines represent sphere 1 and thin lines represent sphere 2) sedimenting in a shear flow with $\hat{\gamma} = -0.05$ and making contact ($\hat{\epsilon} = 0.015$). Initial values of $\hat{r}$, ψ and θ are 30, 0.573° and 45°, respectively.

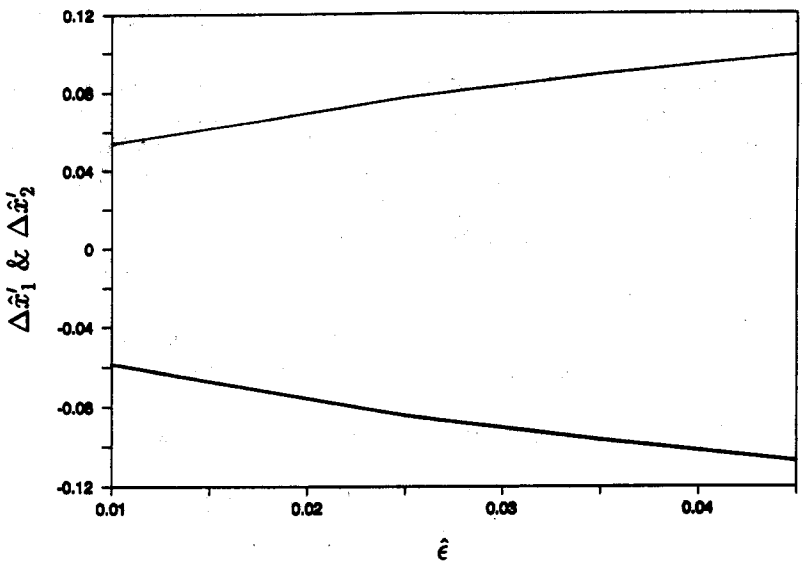

Figure 9. Variations of the net horizontal displacements $\Delta\hat{x}_\alpha'$ of two equal sedimenting spheres ($\lambda = 1$ and $\kappa = 4$) in a shear flow ($\hat{\gamma} - 0.05$) vs their roughness height $\hat{\epsilon}$. The thick line represents $\Delta\hat{x}_1'$ and the thin line represents $\Delta\hat{x}_2'$. Initial values of $\hat{r}$, ψ and θ are 30, 0.573° and 45°, respectively.

figure 9, in which it is observed that the absolute values of the net displacements of the spheres (i.e. $|\Delta\hat{x}_\alpha'|$) increase with their surface roughness height.

5. CONCLUSIONS

The effects of the surface roughness of two spheres sedimenting in a stagnant flow and in a shear flow on their trajectories are calculated. These trajectories are symmetric about a horizontal plane and the spheres undergo no horizontal displacement (as a result of their interactions) when the spheres do not make physical contact during their sedimentation (see figures 3 and 6), as is to be expected as a result of the linearity of the equations and boundary conditions. However, the "nonlinear" effect of physical contact between the spheres due to surface roughness eliminates the symmetry of the trajectories and also results in net horizontal displacements of the spheres as a result of their interactions (see figures 5 and 8). This gives a possible physical mechanism by which particles can move horizontally during their sedimentation process and due to shear flow. It can therefore be an important process in a number of phenomena which require such horizontal particle motion. These include the horizontal motion of particles resulting in the formation of vertical columns in bidisperse suspensions (Weiland *et al.* 1984; Batchelor & Janse Van Rensburg 1986) and the diffusion-like motion of particles across the flow in sheared suspensions (Karnis *et al.* 1966). In fact, an investigation of the behavior of dilute bidisperse suspensions using the present results, will be presented in a subsequent publication. The effects of other forces (e.g. van der Waals, double-layer forces etc.) on the trajectories of hydrodynamically interacting spheres can also be modeled by the above theory by ascribing to the spheres an *equivalent roughness*. However, such a simplification is only valid if the length scale over which these forces act is very much smaller than the spheres' radii.

REFERENCES

BATCHELOR, G. K. & GREEN, J. T. 1972 The determination of the bulk stress in a suspension of spherical particles to order c^2. *J. Fluid Mech.* **56,** 401–427.

BATCHELOR, G. K. & JANSE VAN RENSBURG, R. W. 1986 Structure formation in bidisperse sedimentation. *J. Fluid Mech.* **166,** 379–407.

GOLDMAN, A. J., COX, R. G. & BRENNER, H. 1966 The slow motion of two identical arbitrarily oriented spheres through a viscous fluid. *Chem. Engng Sci.* **21,** 1151–1170.

HAPPEL, J. & BRENNER, H. 1965 *Low Reynolds Number Hydrodynamics*. Prentice–Hall, Englewood Cliffs, N.J.

JEFFREY, D. J. & ONISHI, Y. 1984 Calculation of the resistance and mobility functions for two unequal spheres in low-Reynolds-number flow. *J. Fluid Mech.* **139,** 261–290.

KARNIS, A., GOLDSMITH, H. L. & MASON, S. G. 1966 The kinetics of flowing dispersions, I. Concentrated suspensions of rigid particles. *J. Colloid Interface Sci.* **22,** 531–553.

KIM, S. & MIFFLIN, R. T. 1985 The resistance and mobility functions of two equal spheres in low-Reynolds-number flow. *Phys. Fluids* **28,** 2033–2045.

LIN, C. J., LEE, K. J. & SATHER, N. F. 1970 Slow motion of two spheres in a shear field. *J. Fluid Mech.* **43,** 35–47.

OKAGAWA, A., COX, R. G. & MASON, S. G. 1973 The kinetics of flowing dispersions, VI. Transient orientation and rheological phenomena of rods and discs in shear flow. *J. Colloid Interface Sci.* **45,** 303–329.

STIMSON, M. & JEFFERY, G. B. 1926 The motion of two spheres in viscous fluid. *Proc. R. Soc. Lond.* **A111,** 110–116.

WEILAND, R. H., FESSAS, Y. P. & RAMARAO, B. V. 1984 On instability arising during sedimentation of two-component mixtures of solids. *J. Fluid Mech.* **142,** 383–389.

APPENDIX A

Sedimentation of a Dumb-bell with $\boldsymbol{U} = 0$

In this appendix the explicit forms of the coefficients used in [16a–j] are given as follows:

$$K_T = \frac{K_1' K_4' - K_2' K_3'}{K_1' - K_3'} \qquad [A.1]$$

and

$$K_Q = \frac{K_4' - K_2'}{K_1' - K_3'}, \qquad [A.2]$$

where

$$K_1' = \left\{ -y_{21}^b + \frac{\left(1+\frac{1}{\lambda}\right)^2}{4} y_{22}^b + y_{21}^c \left(\frac{1-\lambda}{1+\lambda}\right) + \frac{\left(1+\frac{1}{\lambda}\right)^3}{8} y_{22}^c \left[\frac{\hat{r}}{2} - \frac{1-\lambda}{2(1+\lambda)}\right] + \frac{(1+\lambda)^2}{4} y_{11}^b - y_{12}^b \right.$$

$$\left. - \frac{(1+\lambda)^3}{8} y_{11}^c \left[\frac{\hat{r}}{2} + \frac{1-\lambda}{2(1+\lambda)}\right] \right\} \Bigg/ \frac{(1+\lambda)^3}{8} y_{11}^c - 2y_{21}^c + \frac{\left(1+\frac{1}{\lambda}\right)^3}{8} y_{22}^c,$$

$$K_2' = \frac{y_{21}^b \hat{F}_g^{(1)} + \frac{\left(1+\frac{1}{\lambda}\right)^2}{4} y_{22}^b \hat{F}_g^{(2)} - \frac{(1+\lambda)^2}{4} y_{11}^b \hat{F}_g^{(1)} - y_{12}^b \hat{F}_g^{(2)}}{\frac{(1+\lambda)^3}{8} y_{11}^c - 2y_{21}^c + \frac{\left(1+\frac{1}{\lambda}\right)^3}{8} y_{22}^c},$$

$$K_3' = \left\{ \frac{1+\lambda}{6} y_{11}^a - \tfrac{1}{3} y_{21}^a - \frac{(1+\lambda)^2}{4} y_{11}^b \left[\frac{\hat{r}}{2} + \frac{1-\lambda}{2(1+\lambda)} \right] - y_{21}^b \left[\frac{\hat{r}}{2} - \frac{1-\lambda}{2(1+\lambda)} \right] - \hat{r} \frac{(1+\lambda)^2}{4} y_{11}^b + \hat{r} y_{21}^b \right.$$

$$+ \hat{r} \frac{(1+\lambda)^3}{8} y_{11}^c \left[\frac{\hat{r}}{2} + \frac{1-\lambda}{2(1+\lambda)} \right] + \hat{r} y_{21}^c \left[\frac{\hat{r}}{2} - \frac{1-\lambda}{2(1+\lambda)} \right] - \tfrac{1}{3} y_{21}^a + \frac{\left(1+\frac{1}{\lambda}\right)}{6} y_{22}^a$$

$$\left. + y_{12}^b \left[\frac{\hat{r}}{2} + \frac{1-\lambda}{2(1+\lambda)} \right] + \frac{\left(1+\frac{1}{\lambda}\right)^2}{4} y_{22}^b \left[\frac{\hat{r}}{2} - \frac{1-\lambda}{2(1+\lambda)} \right] \right\}$$

$$\Bigg/ \left[-y_{12}^b + \frac{\left(1+\frac{1}{\lambda}\right)^2}{4} y_{22}^b + \frac{(1+\lambda)^2}{4} y_{11}^b - y_{21}^b - \hat{r} \frac{(1+\lambda)^3}{8} y_{11}^c + \hat{r} y_{21}^c \right]$$

and

$$K_4' = \frac{-\frac{1+\lambda}{6} y_{11}^a \hat{F}_g^{(1)} - \tfrac{1}{3} y_{21}^a \hat{F}_g^{(2)} + \hat{r} \frac{(1+\lambda)^2}{4} y_{11}^b \hat{F}_g^{(1)} + \hat{r} y_{12}^b \hat{F}_g^{(2)} + \tfrac{1}{3} y_{21}^a \hat{F}_g^{(1)} + \frac{1+\frac{1}{\lambda}}{6} y_{22}^a \hat{F}_g^{(2)}}{-y_{12}^b + \frac{\left(1+\frac{1}{\lambda}\right)^2}{4} y_{22}^b + \frac{(1+\lambda)^2}{4} y_{11}^b - y_{21}^b - \hat{r} \frac{(1+\lambda)^3}{8} y_{11}^c + \hat{r} y_{21}^c}.$$

Also

$$K_N = \frac{x_{21}^a \hat{F}_g^{(1)} + \frac{1+\frac{1}{\lambda}}{6} x_{22}^a \hat{F}_g^{(2)} - \frac{1+\lambda}{6} x_{11}^a \hat{F}_g^{(1)} - \tfrac{1}{3} x_{21}^a \hat{F}_g^{(2)}}{-\frac{1+\lambda}{6} x_{11}^a + \tfrac{2}{3} x_{21}^a - \frac{1+\frac{1}{\lambda}}{6} x_{22}^a}, \qquad \text{[A.3]}$$

$$B_1 = K_T \left[-\frac{(1+\lambda)^2}{4} y_{11}^b + y_{21}^b \right] + K_Q \left\{ \frac{1+\lambda}{6} y_{11}^a - \tfrac{1}{3} y_{21}^a \right.$$

$$\left. - \frac{(1+\lambda)^2}{4} y_{11}^b \left[\frac{\hat{r}}{2} + \frac{1-\lambda}{2(1+\lambda)} \right] - y_{21}^b \left[\frac{\hat{r}}{2} - \frac{1-\lambda}{2(1+\lambda)} \right] \right\} - \frac{1+\lambda}{6} y_{11}^a \hat{F}_g^{(1)} - \tfrac{1}{3} y_{21}^a \hat{F}_g^{(2)}, \qquad \text{[A.4]}$$

$$C_1 = -\frac{1+\lambda}{6} x_{11}^a (K_N - \hat{F}_g^{(1)}) + \tfrac{1}{3} x_{21}^a (K_N + \hat{F}_g^{(2)}), \qquad \text{[A.5]}$$

$$B_2 = K_T \left[-y_{12}^b + \frac{\left(1+\frac{1}{\lambda}\right)^2}{4} y_{22}^b \right] + K_Q \left\{ \tfrac{1}{3} y_{21}^a - \frac{\left(1+\frac{1}{\lambda}\right)}{6} y_{22}^a - y_{12}^b \left[\frac{\hat{r}}{2} + \frac{1-\lambda}{2(1+\lambda)} \right] \right.$$

$$\left. - \frac{\left(1+\frac{1}{\lambda}\right)^2}{4} y_{22}^b \left[\frac{\hat{r}}{2} - \frac{1-\lambda}{2(1+\lambda)} \right] \right\} - \tfrac{1}{3} y_{21}^a \hat{F}_g^{(1)} - \frac{\left(1+\frac{1}{\lambda}\right)}{6} y_{22}^a \hat{F}_g^{(2)}, \qquad \text{[A.6]}$$

$$C_2 = \tfrac{1}{3} x_{21}^a (K_N - \hat{F}_g^{(1)}) + \frac{1+\frac{1}{\lambda}}{6} x_{22}^a (K_N + \hat{F}_g^{(2)}) \qquad \text{[A.7]}$$

and

$$A = K_T\left[\frac{(1+\lambda)^3}{8}y^c_{11} - y^c_{21}\right] + K_Q\left\{-\frac{(1+\lambda)^2}{4}y^b_{11} + y^b_{12}\right.$$
$$\left. + \frac{(1+\lambda)^3}{8}y^c_{11}\left[\frac{\hat{r}}{2} + \frac{1-\lambda}{2(1+\lambda)}\right] + y^c_{21}\left[\frac{\hat{r}}{2} - \frac{1-\lambda}{2(1+\lambda)}\right]\right\}. \quad [A.8]$$

In these relations the mobility functions $x^a_{\alpha\beta}$, $y^a_{\alpha\beta}$, $y^b_{\alpha\beta}$ and $y^c_{\alpha\beta}$ are the elements of the necessary mobility tensors in [9], which may be shown to have the forms

$$\hat{a}^{(\alpha\beta)}_{ij} = x^a_{\alpha\beta}e_ie_j + y^a_{\alpha\beta}(\delta_{ij} - e_ie_j),$$
$$\hat{b}^{(\beta\alpha)}_{ji} = \hat{b}^{(\alpha\beta)}_{ij} = y^b_{\alpha\beta}\epsilon_{ijk}e_k$$

and

$$\hat{c}^{(\alpha\beta)}_{ij} = x^c_{\alpha\beta}e_ie_j + y^c_{\alpha\beta}(\delta_{ij} - e_ie_j),$$

where the summation convention is used and δ_{ij} is the Kronecker delta function, ϵ_{ijk} is the permutation symbol and $e_i = (0, 0, 1)$ is the unit vector along the line joining the sphere centers.

APPENDIX B

Sedimentation of a Dumb-bell with $U \neq 0$

In this appendix the explicit forms of the coefficients used in [25a–n] are given as follows:

$$K_{T2} = \frac{(y^b_{11} + y^b_{12})(\hat{F}^{(1)}_g + \hat{F}^{(2)}_g)}{2(y^c_{21} - y^c_{11})}, \quad [B.1]$$

$$K_1 = \left[\frac{y^a_{11}}{3}(\hat{F}^{(2)}_g - \hat{F}^{(1)}_g) + \frac{y^a_{21}}{3}(\hat{F}^{(1)}_g - \hat{F}^{(2)}_g) + \hat{r}y^b_{11}\hat{F}^{(1)}_g - U^{(1)} + \hat{r}y^b_{12}\hat{F}^{(2)}_g + \hat{r}(y^c_{11} - y^c_{21})K_{T2}\right.$$
$$\left. + U^{(2)}\right] \Big/ \left[\tfrac{2}{3}(y^a_{21} - y^a_{11}) + 2\hat{r}(y^b_{11} - y^b_{12}) - \frac{\hat{r}^2}{2}(y^c_{11} + y^c_{21})\right], \quad [B.2]$$

$$K_2 = \frac{(y^g_{11} - y^g_{12})\hat{\gamma} + \hat{r}(y^h_{11} + y^h_{12})\hat{\gamma}}{\tfrac{2}{3}(y^a_{21} - y^a_{11}) + 2\hat{r}(y^b_{11} - y^b_{12}) - \frac{\hat{r}^2}{2}(y^c_{11} + y^c_{21})}, \quad [B.3]$$

$$K_3 = -\frac{\frac{\hat{r}\hat{\gamma}}{2}}{\tfrac{2}{3}(y^a_{21} - y^a_{11}) + 2\hat{r}(y^b_{11} - y^b_{12}) - \frac{\hat{r}^2}{2}(y^c_{11} + y^c_{21})}, \quad [B.4]$$

$$K_4 = \frac{(2y^g_{22} + 2y^g_{12} - \hat{r}y^h_{11} - \hat{r}y^h_{21})\hat{\gamma} + \hat{r}\frac{\hat{\gamma}}{2}}{-\tfrac{2}{3}y^a_{11} + \tfrac{2}{3}y^a_{21} - 2\hat{r}y^b_{12} + 2\hat{r}y^b_{11} - \frac{\hat{r}^2}{2}(y^c_{11} + y^c_{21})}, \quad [B.5]$$

$$K_5 = \frac{\hat{F}^{(1)}_g - \hat{F}^{(2)}_g}{2} - \frac{3(U^{(2)} - U^{(1)})}{2(x^a_{12} - x^a_{11})}, \quad [B.6]$$

$$K_6 = \frac{3\hat{\gamma}(x^g_{12} + x^g_{22})}{2(x^a_{12} - x^a_{11})}, \quad [B.7]$$

$$E^{(1)}_1 = \left(\tfrac{1}{3}y^a_{11} - \tfrac{1}{3}y^a_{21} - \frac{\hat{r}}{2}y^b_{11} - \frac{\hat{r}}{2}y^b_{21}\right)K_1 + (y^b_{21} - y^b_{11})K_{T2} - \tfrac{1}{3}y^a_{11}\hat{F}^{(1)}_g - \tfrac{1}{3}y^a_{21}\hat{F}^{(2)} - U^{(1)}, \quad [B.8]$$

$$E^{(1)}_2 = \left(\tfrac{1}{3}y^a_{11} - \tfrac{1}{3}y^a_{21} - \frac{\hat{r}}{2}y^b_{11} - \frac{\hat{r}}{2}y^b_{21}\right)K_2 + (y^g_{11} + y^g_{21})\hat{\gamma}, \quad [B.9]$$

$$E_3^{(1)} = \left(\tfrac{1}{3}y_{11}^a - \tfrac{1}{3}y_{21}^a - \frac{\hat{r}}{2}y_{11}^b - \frac{\hat{r}}{2}y_{21}^b\right)K_3, \qquad \text{[B.10]}$$

$$F_1 = \left(\tfrac{1}{3}y_{11}^a - \tfrac{1}{3}y_{21}^a - \frac{\hat{r}}{2}y_{11}^b - \frac{\hat{r}}{2}y_{21}^b\right)K_4 - (y_{11}^g + y_{21}^g)\hat{\gamma}, \qquad \text{[B.11]}$$

$$G_1^{(1)} = (\tfrac{1}{3}x_{21}^a - \tfrac{1}{3}x_{11}^a)K_5 + x_{11}^a\hat{F}_g^{(1)} + x_{21}^a\hat{F}_g^{(2)} + U^{(1)}, \qquad \text{[B.12]}$$

$$G_2^{(1)} = -(\tfrac{1}{3}x_{21}^a + \tfrac{1}{3}x_{11}^a)K_6 + 2(x_{11}^g + x_{21}^g)\hat{\gamma}, \qquad \text{[B.13]}$$

$$H_1 = \left(y_{12}^b - y_{11}^b - \frac{\hat{r}}{2}y_{11}^c + \frac{\hat{r}}{2}y_{21}^c\right)K_1 - (y_{11}^c + y_{21}^c)K_{T2} + y_{11}^b\hat{F}_g^{(1)} + y_{12}^b\hat{F}_g^{(2)}, \qquad \text{[B.14]}$$

$$H_2 = \left(y_{12}^b - y_{11}^b - \frac{\hat{r}}{2}y_{11}^c + \frac{\hat{r}}{2}y_{21}^c\right)K_2 + (y_{11}^h + y_{21}^h)\hat{\gamma}, \qquad \text{[B.15]}$$

$$H_3 = \left(y_{12}^b - y_{11}^b - \frac{\hat{r}}{2}y_{11}^c + \frac{\hat{r}}{2}y_{21}^c\right)K_3 - \frac{\hat{\gamma}}{2_{21}}K_{T2} + y_{11}^b\hat{F}_g^{(1)} + y_{12}^b\hat{F}_g^{(2)}, \qquad \text{[B.16]}$$

$$L_1 = K_4\left[y_{11}^b - y_{12}^b + \frac{\hat{r}}{2}(y_{21}^c - y_{11}^c) - \frac{1-\lambda}{2(1+\lambda)}(y_{11}^c + y_{21}^c) + \hat{\gamma}(y_{11}^h + y_{21}^h) - \frac{\hat{\gamma}}{2}\right], \qquad \text{[B.17]}$$

$$E_1^{(2)} = \left(\tfrac{1}{3}y_{21}^a - \tfrac{1}{3}y_{22}^a - \frac{\hat{r}}{2}y_{12}^b - \frac{\hat{r}}{2}y_{22}^b\right)K_1 + (y_{22}^b - y_{12}^b)K_{T2} - \tfrac{1}{3}y_{21}^a\hat{F}_g^{(1)} - \tfrac{1}{3}y_{22}^a\hat{F}^{(2)} - U^{(2)}, \qquad \text{[B.18]}$$

$$E_2^{(2)} = \left(\tfrac{1}{3}y_{21}^a - \tfrac{1}{3}y_{22}^a - \frac{\hat{r}}{2}y_{12}^b - \frac{\hat{r}}{2}y_{22}^b\right)K_2 + (y_{12}^g + y_{22}^g)\hat{\gamma}, \qquad \text{[B.19]}$$

$$E_3^{(2)} = \left(\tfrac{1}{3}y_{21}^a - \tfrac{1}{3}y_{22}^a - \frac{\hat{r}}{2}y_{12}^b - \frac{\hat{r}}{2}y_{22}^b\right)K_3, \qquad \text{[B.20]}$$

$$F_2 = \left(\tfrac{1}{3}y_{21}^a - \tfrac{1}{3}y_{22}^a - \frac{\hat{r}}{2}y_{12}^b - \frac{\hat{r}}{2}y_{22}^b\right)K_4 - (y_{12}^g + y_{22}^g)\hat{\gamma}, \qquad \text{[B.21]}$$

$$G_1^{(2)} = (\tfrac{1}{3}x_{22}^a - \tfrac{1}{3}x_{21}^a)K_5 + x_{21}^a\hat{F}_g^{(1)} + x_{22}^a\hat{F}_g^{(2)} + U^{(2)} \qquad \text{[B.22]}$$

and

$$G_2^{(2)} = (\tfrac{1}{3}x_{22}^a - \tfrac{1}{3}x_{21}^a)K_6 + 2(x_{12}^g + x_{22}^g)\hat{\gamma} \qquad \text{[B.23]}$$

In these relations the mobility functions $x_{\alpha\beta}^a$, $y_{\alpha\beta}^a$, $y_{\alpha\beta}^b$ and $y_{\alpha\beta}^c$ are as defined in appendix A, whilst the mobility functions $x_{\alpha\beta}^g$, $y_{\alpha\beta}^g$ and $y_{\alpha\beta}^h$ are the elements of the mobility tensors $\hat{g}_{ijk}^{(\alpha)}$ and $\hat{h}_{ijk}^{(\alpha)}$, which may be shown to have the forms

$$\hat{g}_{ijk}^{(\alpha)} = \left(\frac{2}{1+\lambda}\right)^{2-\alpha}\hat{g}_{jki}^{(1\alpha)} + \left(\frac{2\lambda}{1+\lambda}\right)^{\alpha-1}\hat{g}_{jki}^{(2\alpha)}$$

and

$$\hat{h}_{ijk}^{(\alpha)} = \hat{h}_{jkik}^{(1\alpha)} + \hat{h}_{jki}^{(2\alpha)},$$

where

$$\hat{g}_{ijk}^{(\alpha\beta)} = x_{\alpha\beta}^g(e_ie_j - \tfrac{1}{3}\delta_{ij})e_k + y_{\alpha\beta}^g(e_i\delta_{jk} + e_j\delta_{ik} - 2e_ie_je_k)$$

and

$$\hat{h}_{ijk}^{(\alpha\beta)} = y_{\alpha\beta}^h(e_i\epsilon_{jkl}e_l + e_j\epsilon_{ikl}e_l),$$

and where e_l is again the unit vector along the line joining the sphere centers.